HEK293A Cells Memorize a Brief Cold Exposure via a PPARα-Mediated Positive-Feedback Mechanism

Soaad Bader Alfaqaan

Table of Contents

List of Figures

Summary of Abbreviations

ATP	Adenosine Triphosphate
PPARα	Peroxisome Proliferator-activated receptor–alpha
mTORC1	Mammalian target of rapamycin complex-1
D6D	Δ-6 desaturase
PGC1α	Peroxisome proliferator-activated receptor gamma coactivator 1-alpha
LA	Linoleic Acid
AA	Arachidonic Acid
FA	Fatty Acid
PUFA	Polyunsaturated fatty acids
T_F	Final Temperature
MMP	Mitochondrial membrane potential
FAME	Fatty acid methyl ester

Abstract:

Fluctuations in food availability and shifts in temperature are typical environmental changes experienced by animals. These environmental shifts sometimes portend more severe changes and may be indicators for animals to prepare for such a shift. Here I show that mammalian cells, cultured under starvation conditions, can "memorize" a short exposure to cold temperature (15℃) for several days, which was evidenced by their higher survival rate compared to cells continuously grown at 37℃. I refer to this phenomenon as "cold adaptation". The cold-exposed cells retained high ATP levels, and addition of etomoxir, a fatty acid oxidation inhibitor, abrogated the enhanced cell survival. In the standard protocol, cold adaptation required linoleic acid (LA) supplementation along with the activity of Δ-6-desaturase (D6D), a key enzyme in LA metabolism. Moreover, supplementation with the LA metabolite arachidonic acid (AA), which is a high-affinity agonist of peroxisome proliferator-activated receptor-alpha (PPARα), was able to underpin the cold adaptation, even in the presence of a D6D inhibitor. Cold exposure with added LA or AA prompted a surge in PPARα levels, followed by induction of D6D expression; addition of a PPARα antagonist or a D6D inhibitor abrogated both their expression, and reduced cell survival to control levels. I also found that the brief cold exposure transiently prevents PPARα degradation by inhibiting the ubiquitin proteasome system, and starvation contributes to the enhancement of PPARα activity by inhibiting mTORC1. These results reveal an innate adaptive positive-feedback mechanism with a PPARα-D6D-AA axis that is triggered by a brief cold exposure in mammalian cells. "Cold adaptation" could have evolved to increase strength and resilience against imminent extreme cold temperatures.

1. Introduction

1.1 Cooling effects in nature

Environmental stimuli such as cold exposure or chronic dietary changes, influence cellular responses; for instance, energy balance,[1] cell cycle, gene expression, and altered composition or fluidity of lipid membranes.[2-8] It has previously been shown, in both plants and animals, that exposure to cold stimulates an increase in fat utilization to maintain body temperature,[9, 10] alterations in membrane fluidity[11-13] through incorporation of fatty acids into lipid membranes, [14] and activation of the desaturase system,[11] increasing survivability and providing protection from apoptosis.[15] Tolerance to low temperatures is mainly attributed to the unsaturation of membrane lipids.[16] Similarly, energy availability is highly influential to cellular responses and may shift energy metabolism, and trigger alterations in gene expression.

1.2 Therapeutic Cooling

The concept of cooling as a therapeutic tool can be found both in nature and in the medical field. Mammals enter hibernation where metabolic shifts, and cellular responses are altered to maintain survivability. Similarly, medically induced cooling has been employed since the 1950s as a protective means against cerebral injury, where blood flow is reduced.[17] Considerable attention has been paid to the benefits of Therapeutic Hypothermia (TH); a noninvasive therapy with the purpose of decreasing the temperature of structures at risk of damage to 32-34℃ for 72 hours.[18] Previous studies have established that application of this treatment improved health outcomes in post-cardiac arrest [19] and stroke, [20] traumatic brain injury, [21, 22] acute liver failure, [23] and spinal cord injury. [24] In the brain, TH has also been observed to preserve and maintain glucose levels for multiple days' post-trauma through alterations in metabolism,[25, 26] and delayed pro-

inflammatory cytokine production.[27]

Additionally, inhibition of apoptotic pathways and enhanced survivability have been demonstrated in various models. The effect of TH on the caspases pathway possibly makes it the therapeutic measure with the most benefit in preventing neuronal apoptosis,[28-31] and decreasing inflammatory responses.[32] In two independent trials, vascular and neurological performance, along with patient survival were improved by TH, with no adverse side effects.[19, 33] This observation has also been made at a cellular level, where treatment of cells at low temperatures promoted survival.[34] Evidence for a relationship between the glycemic profile in infants with moderate-to-severe hypoxic–ischemic encephalopathy and success of TH has been established, and hints at an association between energy availability and success of TH.[35, 36] Altogether, these studies present known attributes of TH; however the benefits of an acute cold exposure have not yet been fully explored.

1.3 Hibernation and PUFA's

Under energy deprivation, cells alter their metabolism and gene expression patterns. PPARα is a nuclear factor and known master regulator of metabolism responsible for starvation responses and stimulating increases in fat utilization, affecting peroxisomal and mitochondrial ß-oxidation.[37] PPARα may be implicated in disease models such as metabolic syndrome, dyslipidemia, and diabetes.[38-40] In this work, I demonstrate a downstream effect of cold treatment on expression levels of PPARα and ultimately, levels of ß -oxidation, hinting at a possible therapeutic application of cold exposure to increased free fatty acids (FA).

With an interest in cold exposure as an influencer of energy levels, I examined cellular responses, specifically energy levels, to an acute and brief cold exposure. Contrary to the standard

TH therapy duration or the prolonged hibernation phase, the outcomes of a short and drastic drop in temperature have not been thoroughly investigated as a potential intervention. Greater understanding of the molecular mechanisms that underlie the response to cooling at the cellular level will therefore assist these applications. Integrating the concept of TH and the cellular responses and adaptation previously associated with low temperature, I explore the ability of a brief and drastic shift in temperature to enhance cellular viability and identify contributing factors to the observed effects.

1.4 Aims of Thesis

Herein, I explore the ability of a brief and drastic shift in temperature to enhance cellular viability and describe a new method of cellular cooling using a water bath system, by which cells are cooled from 37℃ to 15℃ in approximately 2 min. I uncover a novel relationship between the short cold exposure to maintenance of intracellular ATP levels, mitochondrial membrane potential (MPP) and increased expression of PPARα and D6D leading to enhanced cellular survivability.

2. Materials and Methods

2.1 Materials & Reagents

Materials, reagents, and vendors are as follows: Dulbecco's modified Eagle's medium (DMEM), phenol red-free DMEM, and phosphate buffer saline (-) (PBS) (Nacalai Tesque, Kyoto, Japan); Earle's balanced salt solution without glucose (EBSS) (prepared in the lab according to the recipe from Nacalai Tesque); fetal bovine serum (FBS) (Sigma, St. Louis, MO, USA); linoleic acid sodium salt (Nacalai Tesque); arachidonic acid sodium salt (Nacalai Tesque); penicillin/streptomycin mixed solution (Nacalai Tesque); fatty acid free bovine serum albumin (Nacalai Tesque); cell count reagent SF (Nacalai Tesque); Glo-Lysis buffer (Promega Corporation, Madison, WI, USA); luciferase-based ATP assay kit (Toyo B- net, Tokyo, Japan); 35mm glass-bottom dishes (Mattek, Ashland, MA, USA); 10cm dishes (FPI, Japan); MitoTracker Green FM and Tetramethylrhodamine, ethyl ester (TMRE) (Invitrogen, Carlsbad, CA, USA,); Protein Assay Bicinchoninate Kit (Nacalai Tesque); HEPES (Dojindo, Japan); WY14647, GW6471, MG132, and etomoxir sodium salt (Cayman Chemical, USA); Fatty acid methyl ester mix (Sigma); Fatty acid methyl ester purification kit (06483) and fatty acid ester methylation kit (06482) (Nacalai Tesque); Torin-1 (Funakoshi, Japan); SuperSep Ace 5-20% (Wako, Osaka, Japan).

All chemicals used were of analytical grade and were used as received without any further purification. All solutions were prepared with deionized water.

2.2 Antibodies

Antibodies to phospho-p70 S6 kinase (Thr389) (9234), and p70 S6 kinase (9202) were purchased from Cell Signaling Technology (Danvers, MA, USA); the antibody to PGC1α (NBP1-0467622) was purchased from NovusBio (Littleton CO, USA); the antibody to D6D (ab170665) was from

abcam; the antibody against PPARα (sc-9000) was from Santa Cruz Biotech; antibodies against actin (MAB1501), and against ubiquitin (MAB1510) were from EMD Millipore (Temecula, CA, USA). HRP-labeled secondary antibodies (GE Healthcare UK Ltd., Buckinghamshire, England) were used for visualization by enhanced chemiluminescence (GE Healthcare).

2.3 Cell Culture

HEK293A and HEK293A-ATeam-1.03 cells were cultured in high glucose (450 mg/dL) DMEM, and HepG2 in low glucose (100 mg/dL) DMEM. Cell cultures were supplemented with 10% FBS and maintained at 37℃ and 5% CO_2.

2.4 Starvation and Cold Exposure

HEK293A-ATeam-1.03 cells were plated on 10 cm dishes (FPI, Japan) at a density of 10,000 cells/cm^2 in high glucose DMEM, supplemented with 10% FBS. After 24 h, cells are gently washed twice with PBS and incubated in starvation medium (SM), composed of EBSS supplemented with 20 mM HEPES (pH 7.5), 10 μM linoleic acid sodium salt, 100 unit/mL penicillin, 100 μg/mL streptomycin, and 0.5% fatty acid free-BSA. After a 6 h incubation period in SM, dishes are removed from the incubator and directly placed on a water bath maintained at 5-6℃. The temperature of the medium in the dish was monitored using a sterilized thermometer in a proxy dish. After approximately 2 min on the water bath, the medium reached the desired temperature (15℃) and the plate was immediately placed back into the incubator.

2.5 Cell Viability Assays

Cell viability was determined using SF cell-counting reagent according to the manufacturer's instructions (Nacalai Tesque). Cell viability measurements were carried out using a plate reader (ARVO multi-label counter, Perkin Elmer, Inc.) Cell viability was calculated as the ratio of treated

cells divided by cells cultured under normal conditions in high glucose DMEM. Cell viability was measured from independent trials.

2.6 ATP Luciferase Assay

Cellular ATP concentrations were determined with a luciferase-based ATP assay kit (Toyo B- net) according to the following protocol[41] with slight modifications. Briefly, cells were placed on ice and incubated with Glo-lysis buffer for 5 min. Cell lysates were collected by gentle suspension and combined with the luciferase reagent. Duplicate dishes were prepared for each individual sample, one for the ATP measurement, and one for cell count. ATP measurements were obtained using a luminometer (ARVO multi-label counter), and the cell count was determined using a cell counter (countess II FL, Life technologies). ATP/cell values were calculated by dividing the total ATP amount in the lysate by the total cell number. ATP levels were measured from independent trials.

2.7 Imaging of ATP Concentrations in HEK293A Cells

I first established HEK293A cells continuously expressing ATeam-1.03[42, 43]. Cells were plated at a density of 10,000 cells/cm^2 on a 35mm collagen-coated glass-bottom dish, in phenol red-free DMEM, and the starvation and cold exposure protocols were performed. Imaging was carried out as previously described[44]. Briefly, cells were maintained at 37℃ at 5% CO_2, using a stage top incubator, and illuminated with a 483/32 emission filter for CFP and a 542/27 emission filter for YFP. Data were analyzed using (Molecular Devices, Sunnyvale, CA, USA). The YFP/CFP emission ratio was calculated by dividing YFP intensity by CFP intensity for each cell. ATP levels were measured from independent trials.

2.8 Measurement of Mitochondrial Membrane Potential

HEK293A cells were plated on a 35 mm collagen-coated glass-bottom dish in phenol red-free DMEM. Mitochondria were labeled with 50 nM MitoTracker Green, and 50 nM TMRE to measure mitochondrial membrane potential (MMP). Imaging was carried out according to a previous report[44]. Data were analyzed using MetaMorph analysis software, and the mitochondrial membrane potential per cell was calculated by dividing the average intensities of TMRE by mitochondrial area as determined by signals from Mitotracker Green. MMP was measured from three independent trials.

2.9 Western Blot Analysis

Minimal expression of PPARα was detected in HEK293A-Ateam1.03 cells; thus for Western blot analysis, we overexpressed PPARα to fully visualize the capacity of cold exposure on enhancing PPARα expression (**Supplementary Figure 1**).Cells were collected and lysed in RIPA buffer (150 mM NaCl, 1% NP40, 50 mM Tris-HCl (pH 7.6), 0.1% SDS, 0.5% sodium deoxycholate (Nacalai Tesque) supplemented with 1 mM sodium disphosphate decahydrate, 1 mM NaF, 0.5 mM PMSF, 1 mM NaVO4, 1 × protease inhibitor cocktail (Nacalai Tesque), 10 mM β-glycerophosphate (Sigma), and 0.1% CHAPS (Dojindo, Kumamoto, Japan). After sonication on ice and centrifugation at 4℃ at 15,000 rpm for 15 min, the supernatant was collected, and the protein content was measured using a Protein Assay Bicinchoninate Kit (Nacalai Tesque), following the manufacturer's instructions. Protein samples (35 μg) were prepared, loaded, and separated on SuperSep Ace 5-20% precast gels (Wako), and transferred onto polyvinylidene difluoride (PVDF) membranes (Millipore, Billerica, MA, USA). Western blot analysis detecting ubiquitin was carried out on a 15% gel. Samples taken from three independent trails.

2.10 Fatty Acid Composition Analysis

GC analysis using electron capture detection was used to characterize the fatty acid composition of cell samples. Following the starvation and cold exposure protocols, cells were pelleted by centrifugation at 7,500 rpm for 5 min at 4℃ and counted. Lipids were then extracted by addition of 600 μL cold acetone followed by three rounds of vortexing for 1 min each, freezing with liquid nitrogen, and ultrasonication for 5 min. Cells were then incubated at -20℃ for 1 h, followed by centrifugation at 15,000 rpm at 4℃ for 15 min. The supernatant was collected into a fresh tube and placed on ice. The pellet is resuspended in 400 μL of methanol: water: formic acid (86.5:12.5:1.0), followed by vortexing for 1 min, and 10 min of ultrasonication in a water bath. The sample was placed at -20℃ for 1 h, followed by centrifugation at 15,000rpm at 4℃ for 15 min. The supernatant was collected and combined with the supernatant from the first extraction. The sample was dried under nitrogen followed by methylation and purification using a fatty acid methylation kit, and fatty acid purification kit, respectively (Nacalai Tesque). The sample was injected at a concentration of 1 mg/mL into a GC-MS system consisting of a GCMS-QP2010/Parvum2 (Shimadzu) attached to a DB-5 MS column (Agilent technologies). The flow rate of the Argon gas as a carrier was 1.25 mL/min. Samples taken from three independent trials.

2.11 Transfection

HEK293A-ATeam-1.03 cells were cultured in 10 cm dishes in DMEM supplemented with 10% FBS and incubated at 37℃ for 24 h. The total amount of DNA in each transfection was adjusted to 7.0 μg/dish for 3.1 FLAG-ubiquitin, and 10.5 μg/dish for vector (pcDNA3.1(-)), and pLXSN PPARα-5974. Co-transfections were performed simultaneously with the aforementioned DNA concentrations. Transfections were performed using Lipofectamine 2000 (Life Technologies, Grand Island, NY) according to the manufacturer's recommendations

3. Results

3.1. A brief cold exposure supports cell survival in starvation conditions

As a first step to understanding the effect of cold exposure on cell response, elucidating the optimal parameters of the contributing variables was essential. The time-point and duration of exposure are critical variables to the success of this treatment. Cells were starved in SM supplemented with 10 µM LA, followed by a cold treatment at 2,4,6,8 and 12 hours after the initiation of starvation. Distinct morphological changes were observed in the cells treated with cold, compared to non-treated cells, in that they formed fiber-like structures and maintained a more rounded conformation **Figure 3.1 A**. Morphological distinction and cell viability data indicate that a cold treatment at 4-8 hours after the initiation of starvation is the most effective in triggering a cell survival response. Cell viability was determined by WST assays at 12,24,36, and 48 hours from the time of starvation **Figure 3.1 B**. Treated cells displayed 25% higher cell viability than non-treated cells at 12 hours, a difference that was amplified over the course of 48 hours. Treatment at 6 hours after the initiation of starvation lead to the largest detectible difference in cell viability over a 48-hour period, such that at 36 hours, a difference of 55% is observed between the two conditions. Thus, all further treatments were carried out at this time point.

Along with the time-point, the temperature of the exposure is crucial to this study. Investigating temperature response was carried out by starving cells for 6 hours and exposing cells to cold at different temperatures ranging from 5-25℃. Exposure to temperatures ranging between 10-15℃ were the most effective at enhancing cell survival. WST assays displayed a difference of 25% at 12 hours, and 41% at 36 hours and 51% at 48 hours between exposed and non-exposed cells **Figure 3.1 C**. In addition to the larger temperature shift, a mild cold exposure of 20-25℃ lead to significant morphological and statistical differences in the first 24 hours. A more dramatic change in temperature to a final temperature (T_F) of 15℃ led to statistically relevant outcome over

a 48hr period. From these data, we selected a T_F of 15℃ at 6 hours after the initiation of starvation as the optimal conditions for this treatment.

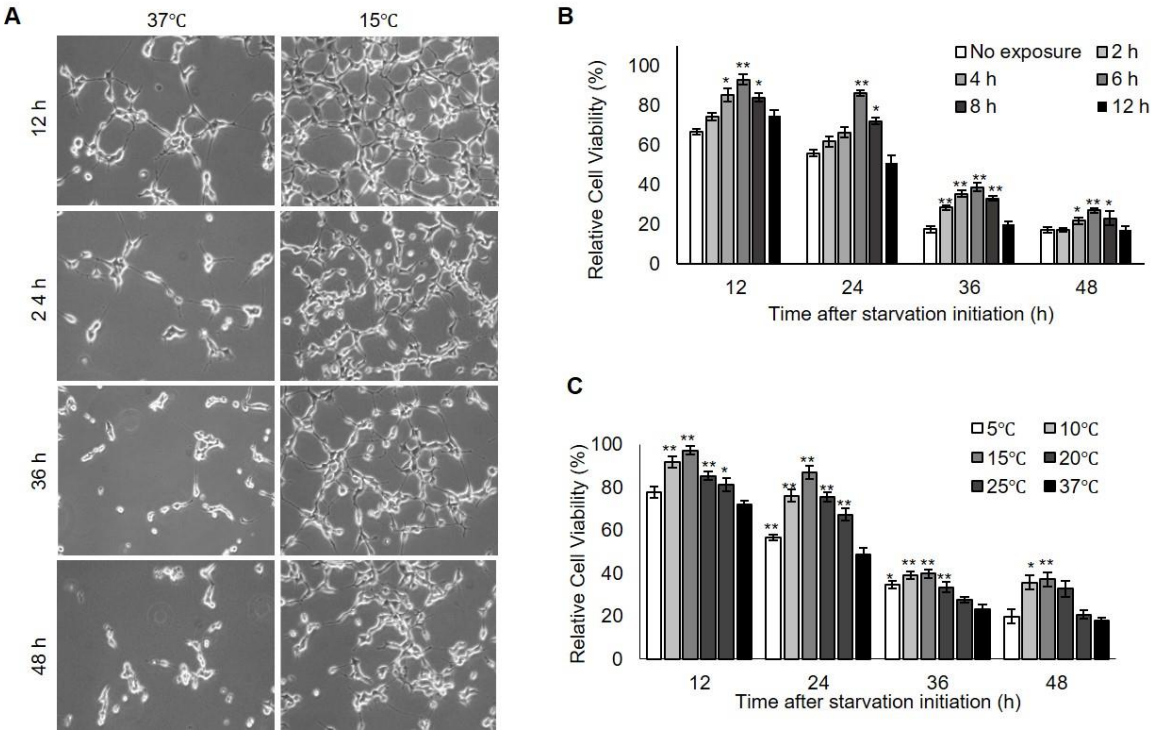

Figure 3.1 (A) Morphology of non-exposed (37℃) and cold-exposed (15℃) cells at various time points after initiation of starvation. Cold exposure was carried out for 2 min at 6 h after initiation of starvation. **(B)** Influence of time of treatment (2 min, 15℃) on cell viability. Cold exposure was carried out at 2, 4, 6, 8, or 12 h after initiation of starvation (*n* = 3). **(C)** Relative cell viability of non-exposed (37℃) and cold-exposed (5-25℃) cells at 6 h after initiation of starvation (*n* =3). Cell viability values of cells cultured in DMEM at 37℃ for 24 h were set as 100%. HEK293A cells were used. Error bars represent SD. **P* <0.05, ***P* <0.01 by unpaired two-tailed Student's t-test.

3.2 A single cold exposure is sufficient to enhance cellular viability

A single exposure to 15ºC at 6 hours' after the initiation of starvation lead to a significant increase in cell viability. However, multiple exposures of 2-3x at various time-points, did not lead to significant differences between single and multiple exposures in **Figure 3.2**. These data indicate that the cold exposure does not possess a cumulative effect, and that a single brief exposure can elicit the cell survival response. Moreover, these data also support that when cold exposure is stimulated multiple times, does not lead to detrimental effects on the cells.

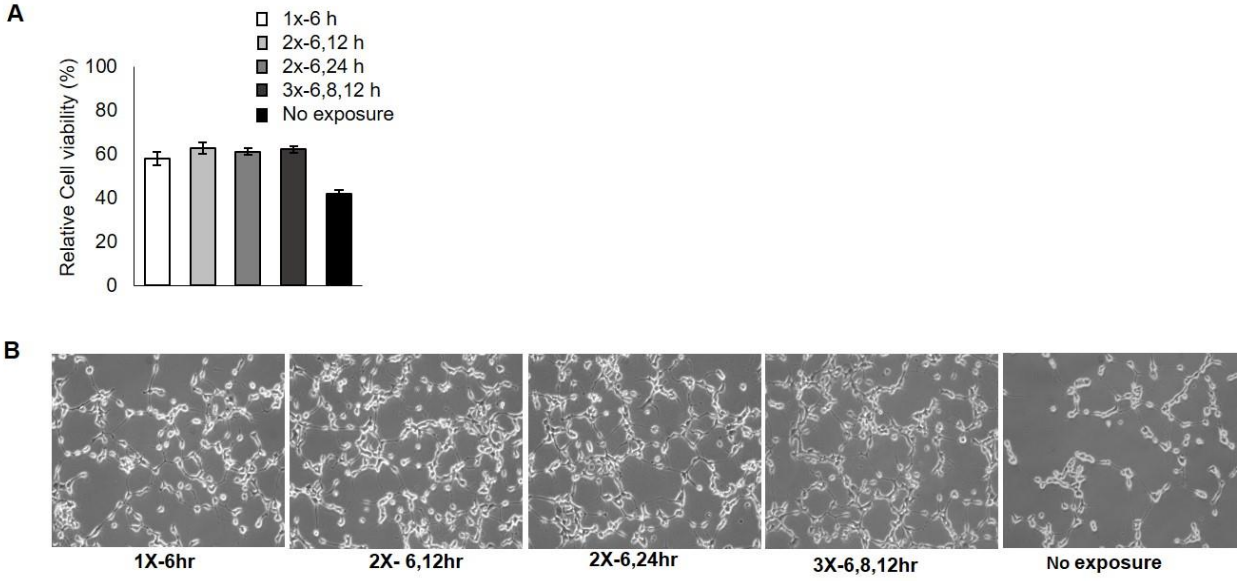

Figure 3.2 Relative cell viability **(A)** and morphology (**B)** of cells treated with a single cold exposure (15℃) at 6 h (1x-6 h), double exposures at 6 and 12 h (2x-6, 12 h), 6 and 24 h (2x-6, 24 h), and triple exposures at 6, 8, and 12 h (3x-6, 8, 12 h) after initiation of starvation, or no exposure (37℃). Cell viability values of cells cultured in DMEM at 37℃ for 24 h were set as 100%. HEK293A cells were used. Error bars represent SD. **P* <0.05, ***P* <0.01 by unpaired two-tailed Student's t-test.

3.3 Cell density highly influences the efficacy of cold exposure

Cellular contiguity is an important influencing factor on cellular responses to particular treatments and environments.[45] The influence of cell density on the effectiveness of the cold exposure was examined by implementing the cold exposure at various cell densities **Figure 3.3**. Cells plated at low densities of 3,000 and 6,000cells/cm^2 did not survive, as cells displayed minimal cell-cell contact. Densities of 10,000 and 20,000 cells/cm^2 displayed the most pronounced outcomes to cold exposure and starvation. At 10,000cells/cm^2, cell viability in exposed cells was 52% greater than in non-exposed cells. However, a cell density of 30,000 cells/cm^2 revealed no differences in cell viability or in morphology between exposed and non-exposed cells. The concept of aggregation effects has been a focus of various studies that have observed how increasing the size or density of a population influences cell signaling and may increase individual survival and fecundity rates.[46-49] A high cell density exhibits little response to cold treatment, and a very low density is unable to survive, therefore, a cell density of 10,000 cells/cm^2 was selected as the most favorable for this treatment.

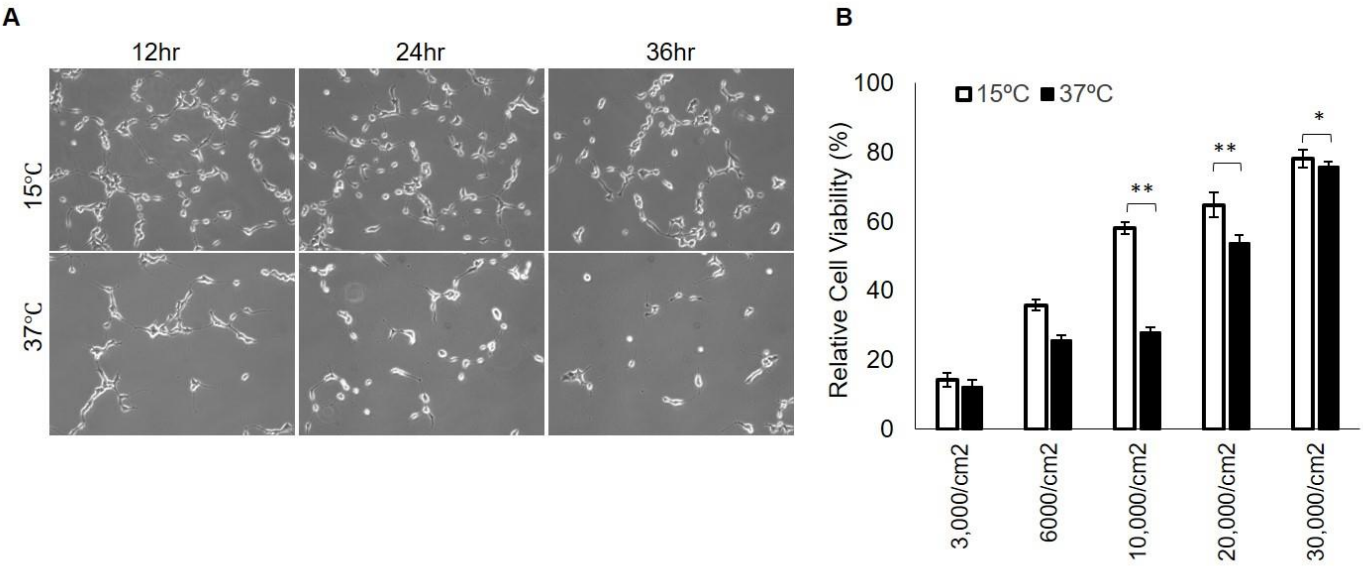

Figure 3.3 (A) Cells grown at 10,000cells/cm^2, starved in SM, and exposed to cold (15°C) at 6 hours after the initiation of starvation, or non-exposed (37°C). **(B)** Cell viability of cells seeded at varying densities and treated at 15°C at 6 hours after the initiation of starvation or non-exposed (37°C). Cell viability values of cells cultured in DMEM at 37°C for 24 h were set as 100%. HEK293A cells were used. Error bars represent SD. **P* <0.05, ***P* <0.01 by unpaired two-tailed Student's t-test.

3.4 pH fluctuation do not contribute to the cold exposure outcome

Fluctuations in pH may cause alterations in cellular response. To minimize the effect of pH change, HEPES was supplemented the culture media. However, to fully eliminate the influence of pH fluctuation as a contributor to the effects of cold exposure, pH fluctuations throughout the experimental protocol were measured, with and without HEPES. Additionally, the cell morphology and cell viability in these conditions was monitored **Figure 3.4**. More pronounced fluctuations in pH were observed in the –HEPES condition, compared to the +HEPES condition during the cold exposure treatment. This indicates that, indeed, pH is altered during the transition of the cells from 37ºC at 5% CO_2 to the water bath, and back. However, comparison of the cell morphology and cell viability demonstrates that the contribution of the change in pH is negligible. These data assure that the increased cell viability and morphological changes are attributed to the cold exposure alone.

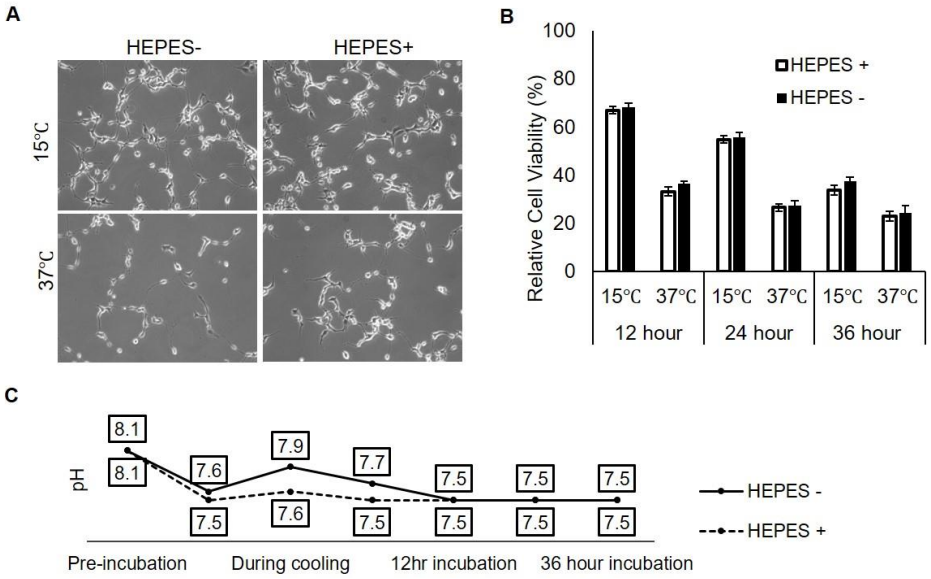

Figure 3.4 (A) Cells starved in SM with HEPES, or without HEPES **(B)** Cell viability of cells starved in SM supplemented with and without HEPES, and treated at 15°C, 37°C. Assay was carried out at 24 hours (*n*=3). **(C)** measurements of the pH of the medium at various time points during the experiment. Cell viability values of cells cultured in DMEM at 37°C for 24 h were set as 100%. HEK293A cells were used. Error bars represent SD. **P* <0.05, ***P* <0.01 by unpaired two-tailed Student's t-test.

3.5 Cold exposure leads to maintained intracellular ATP levels

To measure the intracellular ATP levels, cells were treated as previously described, and imaged at 12, 24, and 36 hours. The intracellular ATP level of individual cells was then determined as a ratio of the YFP/CFP intensities **Figure 3.5 A, B**. Only a 4% decline in the ATP levels was observed between 12-36hours in the treated cells compared to a 44% decline in the non-treated cells. Additionally, ATP levels were further confirmed using a Luciferase based assay **Figure 3.5 C.** The maintained ATP levels correlate with the level of survival in cold treated cells. This indicates that cold exposure causes maintenance of intracellular ATP levels which correlates with increased survivability.

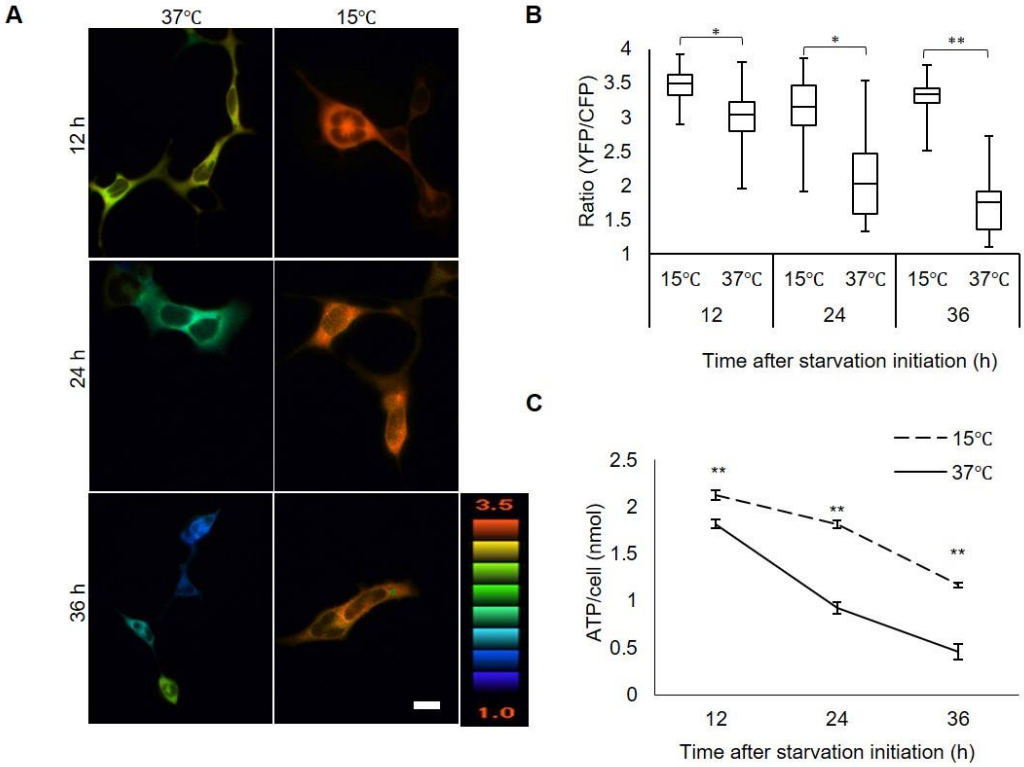

Figure 3.5 (A, B) Measurement of ATP levels by ATeam1.03. **(a)** Visualization of intracellular ATP levels in non-exposed (37°C) and cold-exposed (15°C) cells during starvation. **(b)** Quantification of intracellular ATP levels (measured as the ratio of YFP/CFP). Distribution of data based on the five-number summary: minimum, first quartile, median, third quartile, and maximum (12 h: 15°C, *n* = 92; 37°C, *n* = 111; 24 h: 15°C, *n* = 107; 37°C, *n* = 101; 36 h: 15°C, *n* = 105; 37°C, *n* = 80). Intracellular ATP levels measured by luciferase assays (*n* = 3). Data represent the amount of ATP per cell. **(C)**Intracellular ATP levels of HEK293A cells measured by luciferase assays (*n* = 3). Data represent the amount of ATP per cell.

3.6 Cold exposure sustains mitochondrial membrane activity

Mitochondria play key roles in sensing and reacting to cellular stress, influence cell survival,[50] and a loss of MPP is associated with apoptosis.[51] Thus, I next examined mitochondrial membrane potential using TMRE staining normalized to mitochondrial mass **Figure 3.6**. Consistent with the intracellular ATP levels, MPP levels in non-treated cells experienced a 35% decline, compared a 14% decline in cold treated cells. These data demonstrate a relationship between ATP levels, MPP, and survival.

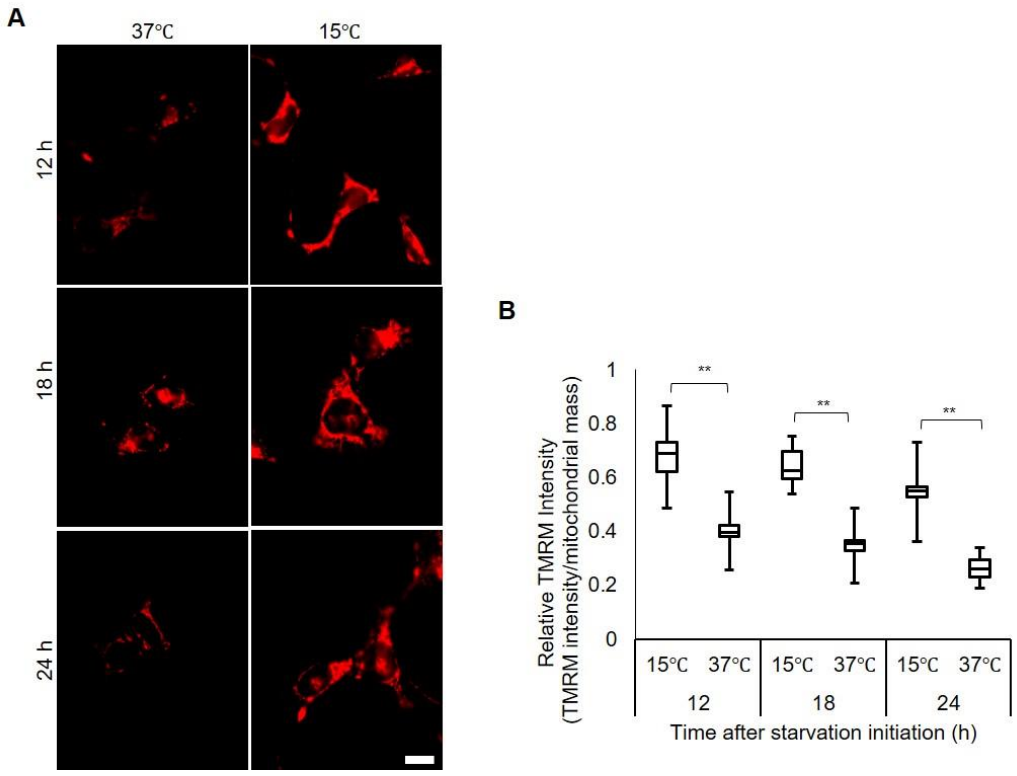

Figure 3.6 (A) Visualization of MMP in non-exposed (37°C) and cold-exposed (15°C) HEK293A cells at 12, 18, and 24 h after initiation of starvation. Scale bar represents 10 μm **(B)** MMP in non-exposed (37°C) and cold-exposed (15°C) cells. Mean values for cells grown continuously in DMEM at 37ºC were set at 1. Distribution of data based on the five-number summary: minimum, first quartile, median, third quartile, and maximum (12 h: 15°C, n = 20 cells; 37°C, n = 13. 18 h: 15°C, n = 42; 37°C, n = 42. 24 h: 15°C, n = 40; 37°C, n = 32). *P <0.05, **P <0.01 by unpaired two-tailed Student's t-test.

3.7 PUFA metabolism and cold exposure are necessary for cell survival

The starvation media used is limited in nutrients and is supplemented with free fatty acid free BSA and LA. Removal of LA from the starvation media ablated the effects of cold treatment in a dose dependent manner **Figure 3.7A, B**. Addition of a minimal amount of LA (1µM) was able to produce the effects of the cold treatment, an effect amplified with increased supplementation **Figure 3.7 B.** These data indicate a direct role for LA in the dynamics of the cold treatment. LA metabolism yields the metabolite AA, through a process that requires the activity of D6D **Figure 3.7 C.** The dependency of this pathway on the rate limiting enzyme (D6D), [52] strongly suggests a role for D6D in cold induced survival.

In addition to its potential as an energy source, LA metabolism yields several metabolites such as arachidonic acid (AA), which serve important biological roles.[53] Thus, I investigated whether LA metabolites are involved in the cold adaptation. To this end, AA was supplemented in place of LA. Like LA, supplementation with AA had similar effects on cell survival and viability **Figure 3.7 D**. Additionally, application of Sc-26196, a specific inhibitor of D6D[54] led to a decrease in cell viability, which was recovered with the supplementation of the downstream metabolite AA **Figure 3.7 D**.

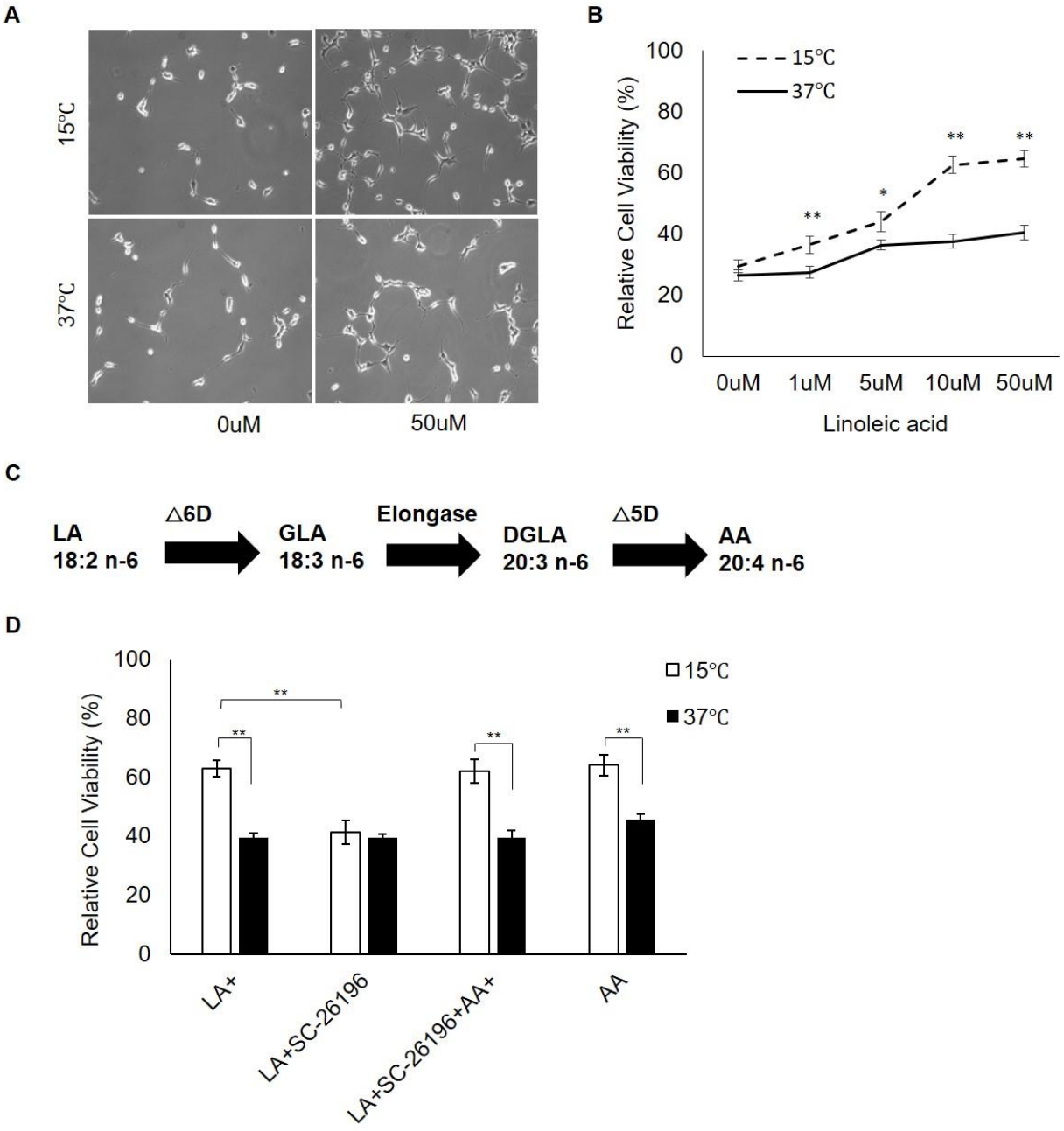

Figure 3.7 (A) Cells grown at 10,000cells/cm^2 and starved in SM and exposed to cold (15°C) or nonexposed (37°C) and treated with or without linoleic acid. Photos taken at 24 hours. **(B)** Dose response of LA supplementation on cell viability of non-exposed (37°C) and cold-exposed (15°C) cells (n = 3). **(C)** schematic of the pathway of LA desaturation by D6D to yield AA**. (D)** Influence of FA supplementation on cell viability of non-exposed (37°C) and cold-exposed (15°C) cells supplemented with 10 μM LA; 10 μM LA +2 μM SC-26196; 10 μM LA +10 μM AA +2 μM SC-26196; and 10 μM AA. (n = 3). HEK293A cells were used. Assays carried out at 24 hours. Cell viability values of cells cultured in DMEM at 37°C for 24 h were set as 100%. Error bars represent SD. *P <0.05, **P <0.01 by unpaired two-tailed Student's t-test.

3.8 Δ-6-desaturase inhibition abrogates the effects of cold treatment

I further investigated the involvement of D6D using Sc-26196 and examining various parameters. Application of the inhibitor mitigated the effects of the cold treatment in a dose dependent manner as determined by cell viability assay **Figure 3.8 A**. Addition of 2-4 μM of the inhibitor lead to no differences between treated and non-treated cells. Similarly, cells were treated with 2 μM of the inhibitor and ATP levels measured using luciferase-based **assays Figure 3.8 B**, and Ateam **Figure 3.8 C, D**. No difference was observed in intracellular ATP between cold treated and non-treated cells, as confirmed by both assays.

FAME analysis of lipid components by GC-MS revealed a large disparity between cold-exposed and non-exposed cells **Figure 3.8 D**. Inhibition of D6D by SC-26196 in cold-exposed cells altered the chromatogram, rendering it similar to that of non-exposed cells. These results further support the notion that cold exposure induces D6D activity, thereby favoring LA metabolism.

3.9 Mitochondrial β-oxidation is implicated in cold exposure

Treatment with etomoxir, a mitochondrial β-oxidation inhibitor, decreased the enhanced cell survival of cold-exposed cells to levels of non-exposed cells **Figure 3.9**. These data support the notion that cold exposure enhances fatty acid oxidation through D6D activity. When considering β-oxidation specifically under starvation conditions, PPARα comes to consideration, specifically in relation to D6D. The previous results demonstrate a clear role for D6D in metabolizing LA into its derivatives, which are known natural high affinity ligands of PPARα.[55, 56] With this idea in mind, I speculated that cold exposure acts as an agonistic ligand for PPARα.

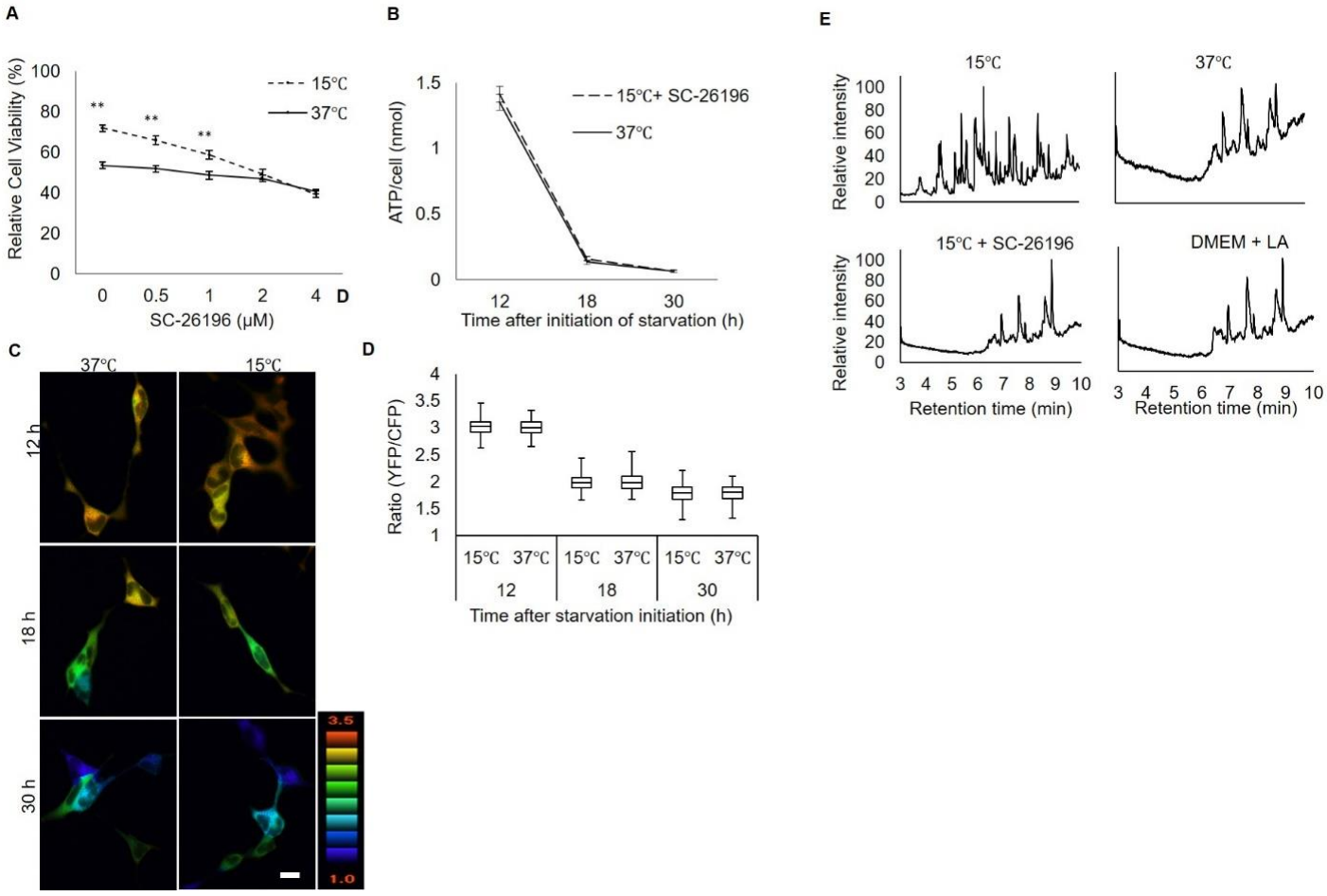

Figure 3.8 (A) Dose response of SC-26196 on cell viability of non-exposed (37℃) and cold-exposed (15℃) cells (n = 3). Assays carried out at 24 h. (**B)** Intracellular ATP levels measured by luciferase assays of non-exposed (37℃) and cold-exposed cells treated with 2 μM SC-26196 (15℃ +SC-26196) (n = 3). **(A, B)** HEK293A cells were used. Cell viability values of cells cultured in DMEM at 37℃ for 24 h were set as 100%. Error bars represent SD. *P <0.05, **P <0.01 by unpaired two-tailed Student's t-test. **(C)** Visualization of intracellular ATP levels in non-exposed (37℃) and cold-exposed (15℃) cells treated with 2 μM SC-26196. SC-26196 was added at 6 h after initiation of starvation. **(D)** Quantification of intracellular ATP levels (measured as the ratio of YFP/CFP). Distribution of data based on the five-number summary: minimum, first quartile, median, third quartile, and maximum from independent trials (12 h: 15℃, n = 113; 37℃, n = 70. 18 h: 15℃, n = 114; 37℃, n = 108. 30 h: 15℃, n = 114; 37℃, n = 105). HEK293A-ATeam1.03 cells were used. Color scale is representative of relative ATP levels. Scale bar represents 10 μm. (**E)** FAME analyses by GC-MS of cold-exposed cells (15℃), non-exposed cells (37℃), cold-exposed cells treated with 2 μM SC-26196 (15℃ + SC-26196), and cells in high glucose DMEM supplemented with 10 μM LA (DMEM + LA). Assays were carried out at 18 h after starvation initiation (n = 3).

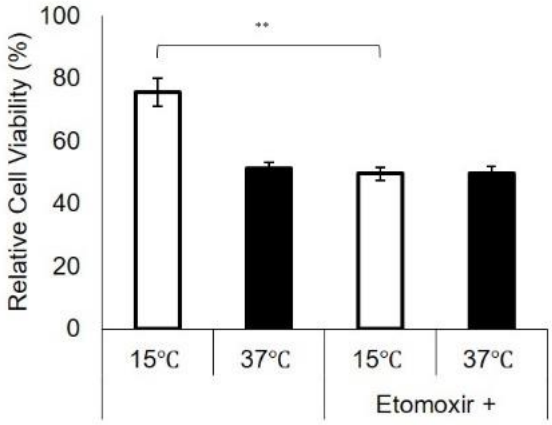

Figure 3.9 Viability of cold-exposed (15°C) or non-exposed (37°C) cells treated with or without 100 μM etomoxir. **Assays** were carried out at 30 h after initiation of starvation. HEK293A cells were used. Cell viability values of cells cultured in DMEM at 37°C for 24 h were set as 100%. Error bars represent SD. *P <0.05, **P <0.01 by unpaired two-tailed Student's t-test.

3.10 Cold exposure enhances PPARα expression and activation

PPARα is a master regulator of fatty acid (FA) metabolism,[38, 57, 58] and it induces genes specific for lipid metabolism, including D6D.[59-62] To understand whether PPARα and D6D are truly implicated in cold exposure, I next measured their expression levels using western blot analysis. I observed PPARα expression from 1 h after the cold exposure, with subsequent D6D expression **Figure 3.10 A**. By contrast, I observed steady-state, constitutive expression of PGC1α, a coactivator or a protein ligand of PPARα,[59, 63] in both cold-exposed and non-exposed cells **Figure 3.10 A.** These results suggest that cold exposure primarily raises the PPARα protein level, promoting its activation through binding to PGC1α.[19] Activated PPARα in turn would induce D6D expression, leading to the production of AA, further activating PPARα.

Consistent with this notion, application of a PPARα antagonist (GW6471) eliminated the expression of D6D along with the cold-induced survival **Figure 3.10 B, C.** Treatment with a PPARα agonist (WY14643) induced both PPARα and D6D expression, even without cold exposure **Figure 3.10 B.** In the presence of LA, I observed continuously increasing PPARα expression along with subsequent D6D induction after the cold exposure **Figure 3.10 A**, however, this pattern was not observed in the absence of LA **Figure 3.10 D.** More interestingly, inhibition of D6D activity eliminated both D6D and PPARα expressions in cold-exposed cells **Figure 3.10 E**. Together, these results point to a positive-feedback mechanism between PPARα and D6D. It is interesting to note that HepG2 cells, derived from a human hepatocellular carcinoma, showed constitutive expression of both PPARα and D6D **Figure 3.10 A**, which is not unexpected in cells that retain many liver-specific characteristics, including fat metabolism.

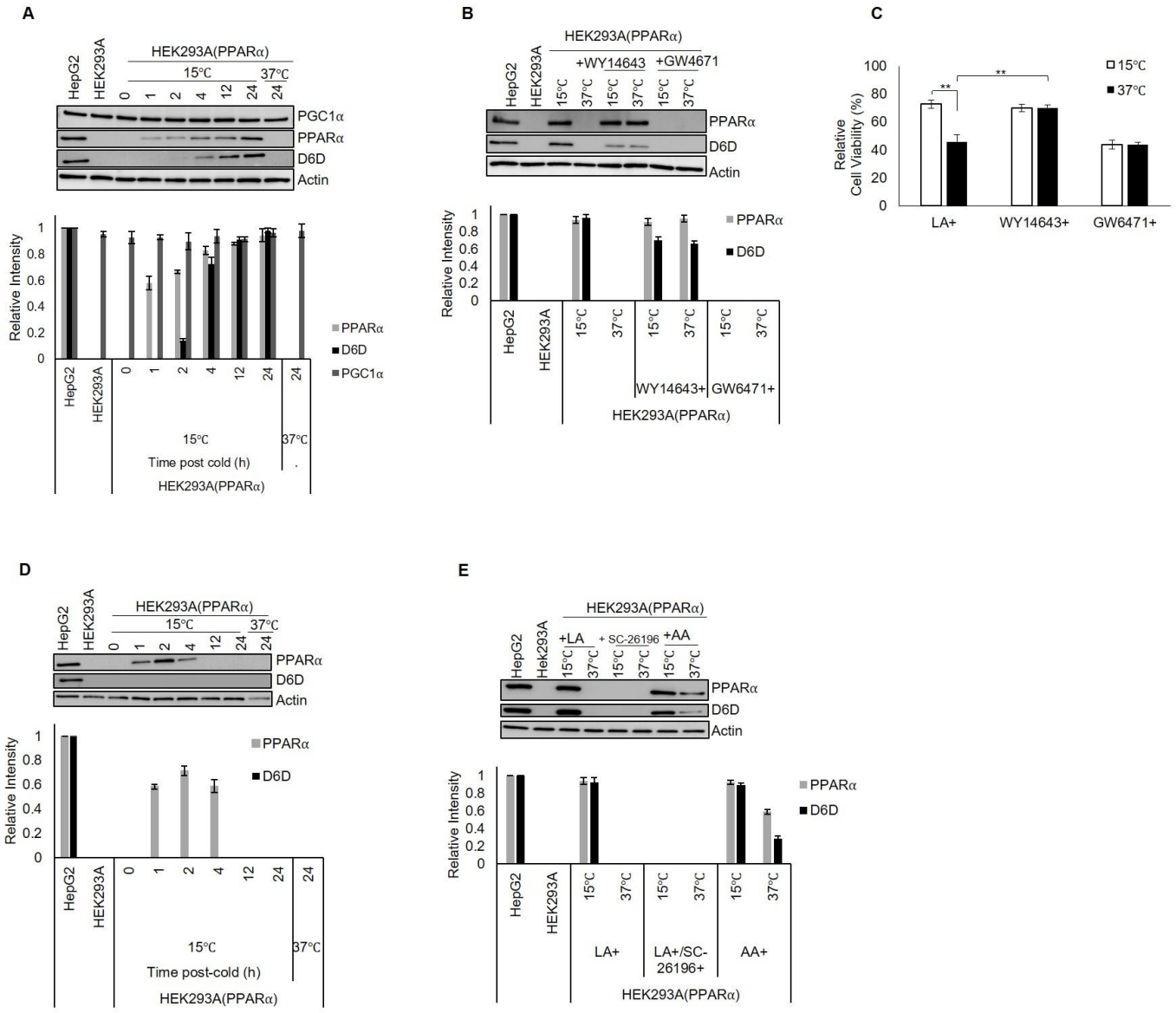

Figure 3.10 (A) Expression of PGC1α, PPARα, and D6D at various time points. Cells were supplemented with 10 μM LA during starvation in non-exposed (37°C) and cold-exposed (15°C) cells. (*n* = 3). **(B, C)** Effects of PPARα agonist (10 μM WY14643) or antagonist (1 μM GW6471) on PPARα and D6D expression levels (**B**) and cell viability (**C**) in non-exposed (37°C) and cold-exposed (15°C) cells. (*n* = 3). **(D)** PPARα and D6D expression at various time points without LA supplementation during starvation in non-exposed (37°C) and cold-exposed (15°C) cells (*n* = 3). **(E)** Influence of FA supplementation on PPARα and D6D expression in non-exposed (37°C) and cold-exposed (15°C) cells supplemented with 10 μM LA; 10 μM LA +2 μM SC-26196; 10 μM AA. (*n* = 3). Cell viability values of HEK293A cells cultured in DMEM at 37°C for 24 h were set as 100%. For western blot analysis, HEK293A(PPARα) were used, and control cells (HEK293A and HepG2) cultured in DMEM at 37°C were harvested 24 h after seeding. Relative protein expression levels were normalized to actin. Values for HepG2 cells were set at 1. Assays for (c, d, e, and g) were carried out at 30 h after initiation of starvation. Error bars represent SD. **P* <0.05, ***P* <0.01 by unpaired two-tailed Student's t-test. For gel source data, see Supplementary Data Fig. 2.

3.11 Cold exposure protects PPARα from UPS mediated degradation

PPARα is readily degraded by the ubiquitin proteasome system (UPS);[64, 65] therefore, I examined PPARα levels in cells treated with MG132, a proteasome inhibitor, and observed sustained PPARα expression in both cold-exposed and non-exposed cells **Figure 3.11 A**, confirming that constitutively translated PPARα is continuously degraded by the UPS. In addition to PPARα expression, D6D expression was also evident in cells treated with MG132 **Figure. 3.11A**, along with downstream FA metabolites, reflecting the presence of D6D activity even in MG132-treated cells maintained at 37ºC **Figure 3.11 B**. Thus, inhibition of the PPARα degradation in non-exposed cells replicates the cold adaptation profile.

I then speculated that cold exposure interferes with the UPS. Indeed, I found a dramatic decrease in the accumulation of ubiquitinated proteins in cold-exposed cells compared to the non-exposed cells **Figure 3.11 C**. Conversely, overexpression of ubiquitin increased the accumulation of ubiquitinated proteins, even in cold-exposed cells **Figure 3.11 C**, eliminated PPARα and D6D expression in cold-exposed cells **Figure 3.11 D**, and abrogated the cold-induced survival **Figure 3.11 E**.

Consistently, cold-exposed cells overexpressing ubiquitin displayed no increase in FA metabolites **Figure 3.11 B**. These results clearly indicate that cold exposure inhibits UPS activity, preventing PPARα degradation. Note that a decrease in ubiquitinated proteins was also observed in cells cultured in DMEM and exposed to cold **Figure 3.11 C**, demonstrating that the ability of a cold exposure to inhibit the UPS is not dependent on a specific nutrient profile.

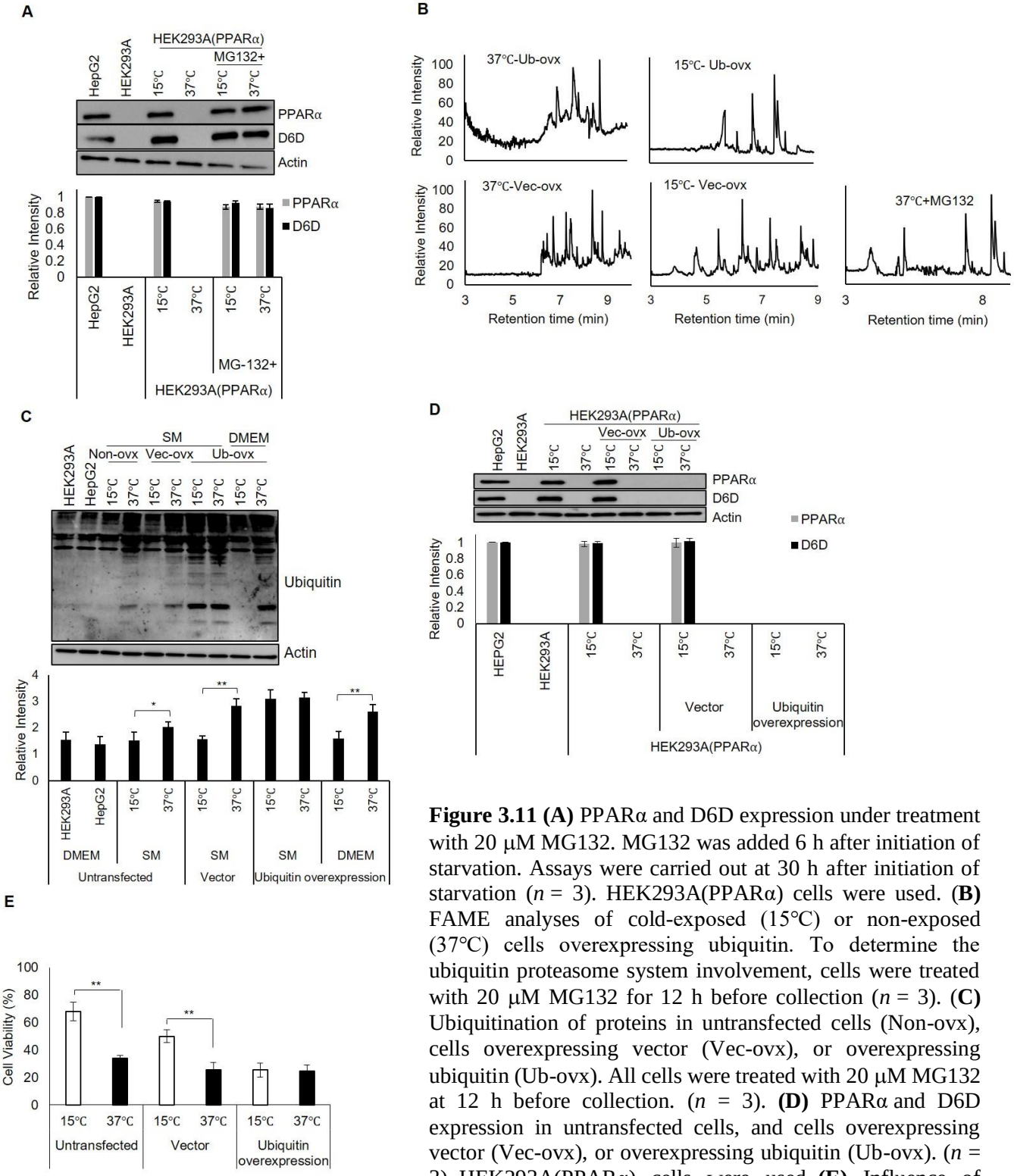

Figure 3.11 (A) PPARα and D6D expression under treatment with 20 μM MG132. MG132 was added 6 h after initiation of starvation. Assays were carried out at 30 h after initiation of starvation (n = 3). HEK293A(PPARα) cells were used. **(B)** FAME analyses of cold-exposed (15°C) or non-exposed (37°C) cells overexpressing ubiquitin. To determine the ubiquitin proteasome system involvement, cells were treated with 20 μM MG132 for 12 h before collection (n = 3). **(C)** Ubiquitination of proteins in untransfected cells (Non-ovx), cells overexpressing vector (Vec-ovx), or overexpressing ubiquitin (Ub-ovx). All cells were treated with 20 μM MG132 at 12 h before collection. (n = 3). **(D)** PPARα and D6D expression in untransfected cells, and cells overexpressing vector (Vec-ovx), or overexpressing ubiquitin (Ub-ovx). (n = 3). HEK293A(PPARα) cells were used. **(E)** Influence of ubiquitin overexpression on cell viability in cold-exposed (15°C) or non-exposed (37°C) cells (n = 3). Cell viability values of cells cultured in DMEM at 37°C for 24 h were set as 100%. Unless stated otherwise, HEK293A were used. Assays for (b, c, d, and e) were carried out at 18 h after initiation of starvation. Control cells (HEK293A and HepG2) cultured in DMEM at 37°C were harvested 24 h after seeding. Relative protein expression levels were normalized to actin. Values for HepG2 cells were set at 1 Error bars represent SD. *P <0.05, **P <0.01 by unpaired two-tailed Student's t-test. For gel source data, see Supplementary Data Fig. 2

3.12 PPARα and D6D expression is limited to low glucose conditions

Cold exposure-induced PPARα and D6D expression was observed under DMEM glucose (-)/LA (+), but not in DMEM glucose (+)/LA (+), glucose (+)/LA (-), or glucose (-)/LA (-) at 24 h post-cold **Figure 3.12 A**. Closer investigation revealed that PPARα and subsequent D6D expression in DMEM glucose (-)/LA (+) were time-dependent **Figure 3.12 B**. Surprisingly, a transient PPARα expression was detected even in DMEM glucose (+)/ LA (+) at only 1 h post-cold **Figure 3.12 C**. D6D, however, was not detected in this condition, implying that continuous expression as well as activation of PPARα does not occur under glucose (+) conditions.

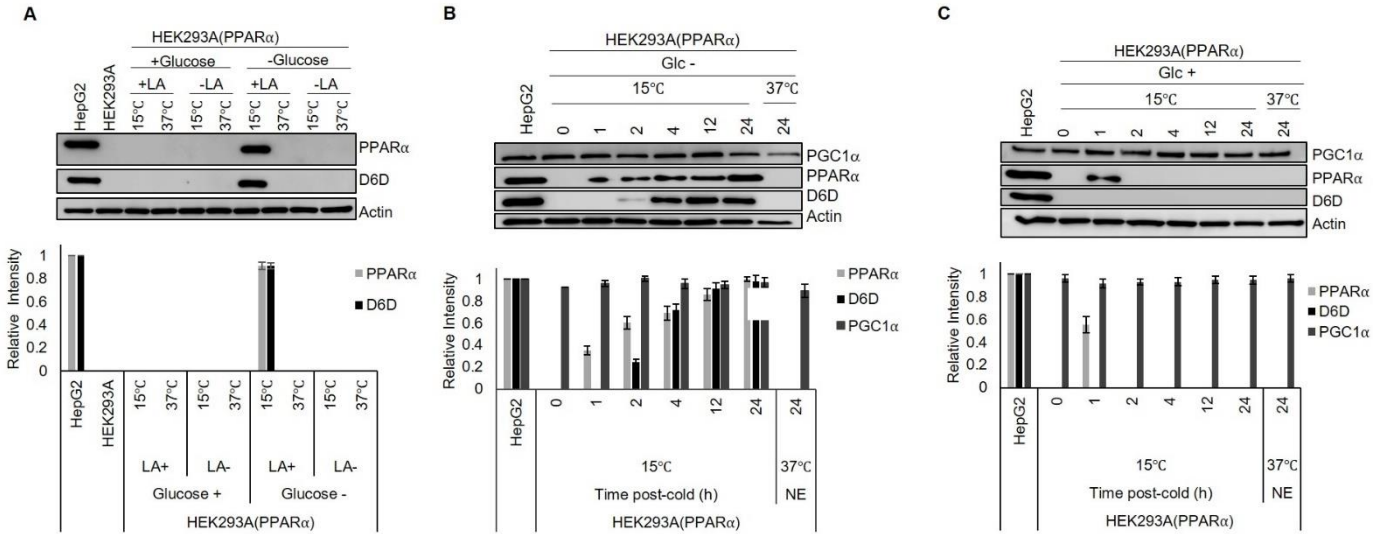

Figure 3.12 (A) PPARα and D6D expressions were limited to glucose (-)/LA (+) conditions. PPARα and D6D expression in cold-exposed (15℃) or non-exposed (37℃) cells treated in DMEM with or without glucose and/or LA supplementation. All cells were collected at 24 h post-treatment. (*n* =3). **(B, C)** Expression levels of PGC1α, PPARα, and D6D at various time points in non-exposed (37℃) and cold-exposed (15℃) cells in DMEM without **(C)** and with **(C)** glucose (*n* = 3). HEK293A(PPARα) cells were used. Control cells (HEK293A and HepG2) cultured in DMEM at 37℃ were harvested 24 h after seeding. Relative protein expression levels were normalized to actin. All blots were derived from individual gels using the same samples. Values for HepG2 cells were set at 1. Error bars represent SD. For gel source data, see Supplementary Data Fig. 2

3.13 Inhibition of mTORC1 under glucose conditions restores PPARα and D6D expression

A previous study revealed that the inhibition of the mammalian target of rapamycin 1 (mTORC1) is required for the activation of PPARα.[66] The activation of mTORC1 is influenced by nutrients such as glucose,[67, 68] and triggers cellular responses by phosphorylating p70 S6 kinase (p70S6K).[69] Consistent with this, addition of Torin-1, an mTORC1 inhibitor, even in DMEM glucose (+) led to clear PPARα and D6D expression after cold exposure **Figure 3.13 A**. Furthermore, glucose doses ranging from 0 to 450 mg/dL showed an inverse relationship between PPARα and S6K phosphorylation levels. Although PPARα and D6D expression was not observed under the high glucose condition (450 mg/dL), both expressions were observed at relatively low glucose concentrations, up to 100 mg/dL glucose, after cold exposure **Figure 3.13 B.**

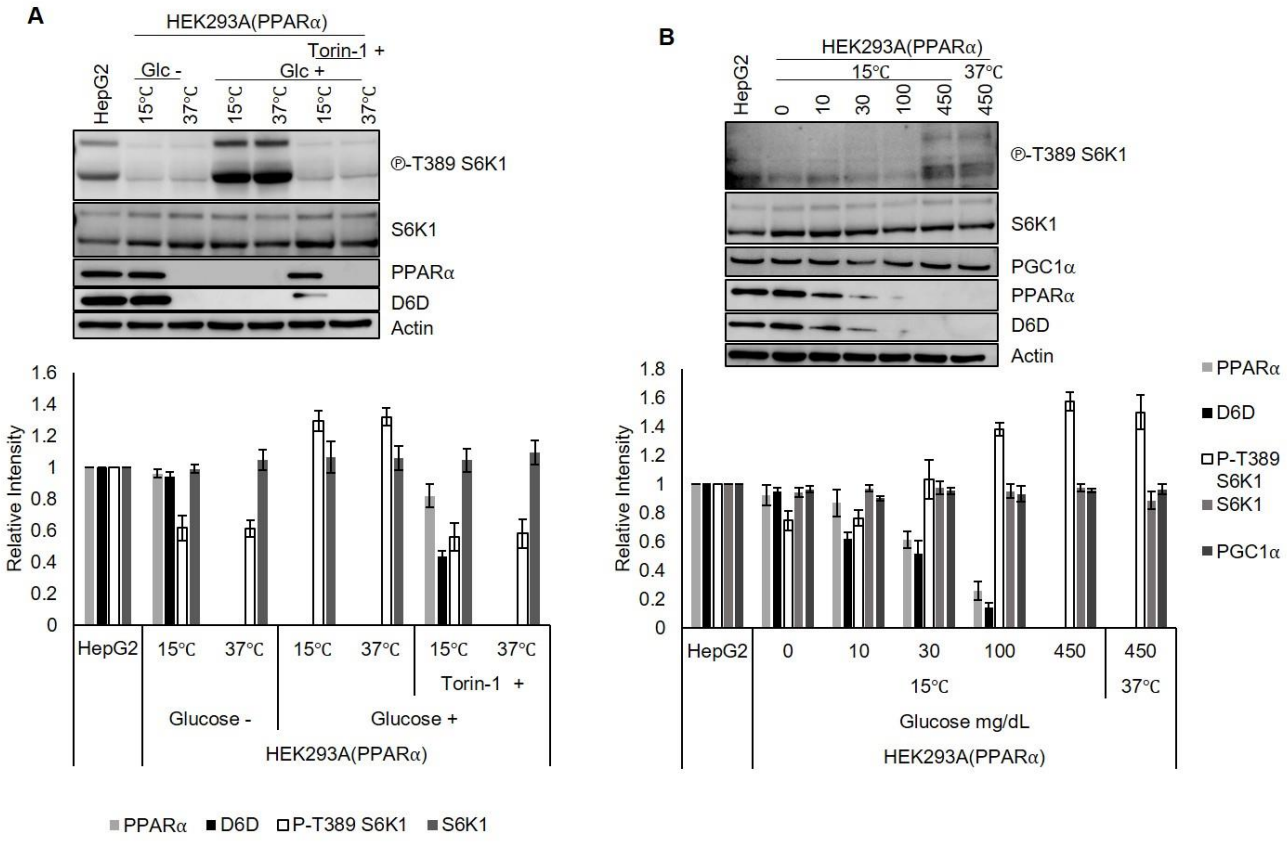

Figure 3.13 (A) PPARα and D6D expression in non-exposed (37°C) and cold-exposed (15°C) cells treated in DMEM with ± glucose, and ± 1 μM Torin-1 (mTORC1 inhibitor). Torin-1 was added 24 hours prior to collection, and cold exposed cells were treated at 18 hours prior to collection (n = 3). **(B)** PPARα and D6D expression under varying doses of glucose (0-450 mg/dL) in cold-exposed (15°C) or non-exposed (37°C) cells. Assays were carried out at 24 h after glucose deprivation (n = 3). HEK293A(PPARα) cells were used. Control cells (HEK293A and HepG2) cultured in DMEM at 37°C were harvested 24 h after seeding. Relative protein expression levels were normalized to actin. Values for HepG2 cells were set at 1. Error bars represent SD. For gel source data, see Supplementary Data Fig. 2

4. Discussion

Herein, I have uncovered a relationship between an acute and brief cold exposure to an increase in PPARα gene expression mediated through a PPARα-D6D-AA positive-feedback loop. During this study cold exposure appears to be initially sensed by the UPS and results in its inhibition, which leads to PPARα stabilization.[46] PPARα then transcriptionally activates genes involved in lipid metabolism, including D6D to produce AA, which further activates PPARα as its high affinity ligand. This gives rise to a positive-feedback loop between PPARα, D6D, and AA. This feedback loop continuously activates lipid metabolism, which is demonstrated by the maintained MPP levels to produce ATP. I refer to this phenomenon as "cold adaptation". Furthermore, these data suggest that starvation further enhances this positive-feedback loop, as the presence of high amounts of glucose attenuates PPARα and D6D expression, and inhibition of mTORC1 was able to reverse this.

Cold exposure results in enhanced cellular dynamics[2] and is associated with modulation of cell metabolism, gene expression, and cellular ATP levels.[70-72] Here I confirm these observations showing that, after cold exposure of cells to 15°C for approximately 2 min., 6 hours post starvation, cells do indeed modulate their metabolism and are capable of withstanding starvation under LA or AA supplementation. Single and multiple cold exposures lead to similar outcomes, indicating that this single exposure is fully capable of eliciting the cold exposure response in cells.

Adaptation is a fundamental survival strategy for organisms to cope with environmental changes and is most typically associated with neurons and the sympathetic nervous system. In this study I found that "cold adaptation" is a more fundamental type of cellular adaptation. HEK293A cells in culture acquire a quasi-stable cellular metabolic state that may be considered a form of cellular memory. In response to a brief exposure to cold in this case, this cellular "memory,"

sustained by a positive-feedback loop enhances cell viability and supports the notion of a fundamental type of cellular adaptation.

While the PPARα-D6D axis has been implicated under various environmental conditions, implication of the UPS by cold exposure leading to the enhancement of PPARα accumulation and activation has not previously been reported. The UPS regulates a multitude of systems. Hence, identifying and understanding the influencers of its activity can contribute to the general knowledge of the UPS itself and its controlling systems, such as cold adaptation. In addition, these data illustrate the presence of a PPARα-D6D-AA positive-feedback mechanism that is triggered by a brief cold exposure. This system may be utilized by mammals in cold seasons or hibernation, in which food is expected to be limited, and in which lipid metabolism is the primary source of fuel. It might be interesting to examine cells from such mammals to further investigate the mechanism driving resilience of cellular metabolic states.

5. References

1. Sonna, L.A., Fujita, J., Gaffin, S.L. & Lilly, C.M. Invited review: Effects of heat and cold stress on mammalian gene expression. *J Appl Physiol (1985)* **92**, 1725-1742 (2002).
2. Fujita, J. Cold shock response in mammalian cells. *J Mol Microbiol Biotechnol* **1**, 243-255 (1999).
3. Sakurai, T. *et al.* Low temperature protects mammalian cells from apoptosis initiated by various stimuli in vitro. *Exp Cell Res* **309**, 264-272 (2005).
4. Chintalapati, S., Kiran, M.D. & Shivaji, S. Role of membrane lipid fatty acids in cold adaptation. *Cell Mol Biol (Noisy-le-grand)* **50**, 631-642 (2004).
5. Murata, N. & Los, D.A. Membrane Fluidity and Temperature Perception. *Plant Physiol* **115**, 875-879 (1997).
6. Nakamura, M.T. & Nara, T.Y. Structure, function, and dietary regulation of Δ6, Δ5, and Δ9 desaturases. *Annu Rev Nutr* **24**, 345-376 (2004).
7. Penfield, S. Temperature perception and signal transduction in plants. *New Phytol* **179**, 615-628 (2008).
8. Solanke, A.U. & Sharma, A.K. Signal transduction during cold stress in plants. *Physiol Mol Biol Plants* **14**, 69-79 (2008).
9. Bing, C. *et al.* Hyperphagia in cold-exposed rats is accompanied by decreased plasma leptin but unchanged hypothalamic NPY. *Am J Physiol* **274**, R62-68 (1998).
10. Luz, J. & Griggio, M.A. Effect of food intake on oxygen consumption in cold-acclimated rats. *Braz J Med Biol Res* **20**, 619-622 (1987).
11. Clarkson, D.T., Hall, K.C. & Roberts, J.K. Phospholipid composition and fatty acid desaturation in the roots of rye during acclimatization of low temperature : Positional analysis of fatty acids. *Planta* **149**, 464-471 (1980).
12. Murata, N. Low-temperature effects on cyanobacterial membranes. *J Bioenerg Biomembr* **21**, 61-75 (1989).
13. Wada, H. & Murata, N. Temperature-Induced Changes in the Fatty Acid Composition of the Cyanobacterium, *Synechocystis* PCC6803. *Plant Physiol* **92**, 1062-1069 (1990).
14. Ashworth, E.N. & Christiansen, M.N. Effect of Temperature and BASF 13 338 on the Lipid Composition and Respiration of Wheat Roots. *Plant Physiol* **67**, 711-715 (1981).

15. Song, S., Bae, D.W., Lim, K., Griffiths, M.W. & Oh, S. Cold stress improves the ability of *Lactobacillus plantarum* L67 to survive freezing. *Int J Food Microbiol* **191**, 135-143 (2014).
16. Wada, H., Gombos, Z. & Murata, N. Contribution of membrane lipids to the ability of the photosynthetic machinery to tolerate temperature stress. *Proc Natl Acad Sci U S A* **91**, 4273-4277 (1994).
17. Knight, J.R. & Willis, A.E. Control of translation in the cold: implications for therapeutic hypothermia. *Biochem Soc Trans* **43**, 333-337 (2015).
18. Shankaran, S. Therapeutic hypothermia for neonatal encephalopathy. *Curr Opin Pediatr* **27**, 152-157 (2015).
19. Group, H.a.C.A.S. Mild therapeutic hypothermia to improve the neurologic outcome after cardiac arrest. *N Engl J Med* **346**, 549-556 (2002).
20. Yenari, M.A. & Hemmen, T.M. Therapeutic hypothermia for brain ischemia: where have we come and where do we go? *Stroke* **41**, S72-74 (2010).
21. Foundation, B.T., Surgeons, A.A.o.N. & Surgeons, C.o.N. Guidelines for the management of severe traumatic brain injury. *J Neurotrauma* **24 Suppl 1**, S1-106 (2007).
22. Guven, H. *et al.* Moderate hypothermia prevents brain stem oxidative stress injury after hemorrhagic shock. *J Trauma* **53**, 66-72 (2002).
23. Stravitz, R.T. & Larsen, F.S. Therapeutic hypothermia for acute liver failure. *Crit Care Med* **37**, S258-264 (2009).
24. Dietrich, W.D. Therapeutic hypothermia for spinal cord injury. *Crit Care Med* **37**, S238-242 (2009).
25. Williams, G.D., Dardzinski, B.J., Buckalew, A.R. & Smith, M.B. Modest hypothermia preserves cerebral energy metabolism during hypoxia-ischemia and correlates with brain damage: a 31P nuclear magnetic resonance study in unanesthetized neonatal rats. *Pediatr Res* **42**, 700-708 (1997).
26. Kimura, T. *et al.* Effect of mild hypothermia on energy state recovery following transient forebrain ischemia in the gerbil. *Exp Brain Res* **145**, 83-90 (2002).
27. Kimura, A., Sakurada, S., Ohkuni, H., Todome, Y. & Kurata, K. Moderate hypothermia delays proinflammatory cytokine production of human peripheral blood mononuclear cells. *Crit Care Med* **30**, 1499-1502 (2002).

28. Zhao, H., Yenari, M.A., Sapolsky, R.M. & Steinberg, G.K. Mild postischemic hypothermia prolongs the time window for gene therapy by inhibiting cytochrome C release. *Stroke* **35**, 572-577 (2004).
29. Zhao, H., Sapolsky, R.M. & Steinberg, G.K. Phosphoinositide-3-kinase/akt survival signal pathways are implicated in neuronal survival after stroke. *Mol Neurobiol* **34**, 249-270 (2006).
30. Zhao, H. *et al.* Conditions of protection by hypothermia and effects on apoptotic pathways in a rat model of permanent middle cerebral artery occlusion. *J Neurosurg* **107**, 636-641 (2007).
31. López-Hernández, F.J., Ortiz, M.A. & Piedrafita, F.J. The extrinsic and intrinsic apoptotic pathways are differentially affected by temperature upstream of mitochondrial damage. *Apoptosis* **11**, 1339-1347 (2006).
32. Schmitt, K.R. *et al.* Hypothermia suppresses inflammation via ERK signaling pathway in stimulated microglial cells. *J Neuroimmunol* **189**, 7-16 (2007).
33. Bernard, S.A. *et al.* Treatment of comatose survivors of out-of-hospital cardiac arrest with induced hypothermia. *N Engl J Med* **346**, 557-563 (2002).
34. Hofmann, S., Cherkasova, V., Bankhead, P., Bukau, B. & Stoecklin, G. Translation suppression promotes stress granule formation and cell survival in response to cold shock. *Mol Biol Cell* **23**, 3786-3800 (2012).
35. Basu, S.K. *et al.* Hypoglycaemia and hyperglycaemia are associated with unfavourable outcome in infants with hypoxic ischaemic encephalopathy: a post hoc analysis of the CoolCap Study. *Arch Dis Child Fetal Neonatal Ed* **101**, F149-155 (2016).
36. Basu, S.K., Salemi, J.L., Gunn, A.J., Kaiser, J.R. & Group, C.S. Hyperglycaemia in infants with hypoxic-ischaemic encephalopathy is associated with improved outcomes after therapeutic hypothermia: a post hoc analysis of the CoolCap Study. *Arch Dis Child Fetal Neonatal Ed* **102**, F299-F306 (2017).
37. Kersten, S. *et al.* Peroxisome proliferator-activated receptor α mediates the adaptive response to fasting. *J Clin Invest* **103**, 1489-1498 (1999).
38. Kersten, S., Desvergne, B. & Wahli, W. Roles of PPARs in health and disease. *Nature* **405**, 421-424 (2000).

39. Agarwal, S., Yadav, A. & Chaturvedi, R.K. Peroxisome proliferator-activated receptors (PPARs) as therapeutic target in neurodegenerative disorders. *Biochem Biophys Res Commun* **483**, 1166-1177 (2017).
40. Dong, C. *et al.* Role of peroxisome proliferator-activated receptors gene polymorphisms in type 2 diabetes and metabolic syndrome. *World J Diabetes* **6**, 654-661 (2015).
41. Yoshida, T., Kakizuka, A. & Imamura, H. BTeam, a Novel BRET-based Biosensor for the Accurate Quantification of ATP Concentration within Living Cells. *Sci Rep* **6**, 39618 (2016).
42. Imamura, H. *et al.* Visualization of ATP levels inside single living cells with fluorescence resonance energy transfer-based genetically encoded indicators. *Proc Natl Acad Sci U S A* **106**, 15651-15656 (2009).
43. Yoshida, T., Alfaqaan, S., Sasaoka, N. & Imamura, H. Application of FRET-Based Biosensor "ATeam" for Visualization of ATP Levels in the Mitochondrial Matrix of Living Mammalian Cells. *Methods Mol Biol* **1567**, 231-243 (2017).
44. Nakano, M. *et al.* ATP Maintenance via Two Types of ATP Regulators Mitigates Pathological Phenotypes in Mouse Models of Parkinson's Disease. *EBioMedicine* **22**, 225-241 (2017).
45. Reuven, N., Adler, J., Meltser, V. & Shaul, Y. The Hippo pathway kinase Lats2 prevents DNA damage-induced apoptosis through inhibition of the tyrosine kinase c-Abl. *Cell Death Differ* **20**, 1330-1340 (2013).
46. Muller, C., Laval, F., Soues, S., Birck, C. & Charcosset, J.Y. High cell density-dependent resistance and P-glycoprotein-mediated multidrug resistance in mitoxantrone-selected Chinese hamster cells. *Biochem Pharmacol* **43**, 2091-2102 (1992).
47. Zi, Z. & Klipp, E. Cellular signaling is potentially regulated by cell density in receptor trafficking networks. *FEBS Lett* **581**, 4589-4595 (2007).
48. Kobayashi, H., Takemura, Y. & Ohnuma, T. Relationship between tumor cell density and drug concentration and the cytotoxic effects of doxorubicin or vincristine: mechanism of inoculum effects. *Cancer Chemother Pharmacol* **31**, 6-10 (1992).
49. Trajkovic, K., Valdez, C., Ysselstein, D. & Krainc, D. Fluctuations in cell density alter protein markers of multiple cellular compartments, confounding experimental outcomes. *PLoS One* **14**, e0211727 (2019).

50. Bravo-Sagua, R. *et al.* Cell death and survival through the endoplasmic reticulum-mitochondrial axis. *Curr Mol Med* **13**, 317-329 (2013).
51. Gottlieb, E., Armour, S.M., Harris, M.H. & Thompson, C.B. Mitochondrial membrane potential regulates matrix configuration and cytochrome *c* release during apoptosis. *Cell Death Differ* **10**, 709-717 (2003).
52. Los, D.A. & Murata, N. Structure and expression of fatty acid desaturases. *Biochim Biophys Acta* **1394**, 3-15 (1998).
53. Bézard, J., Blond, J.P., Bernard, A. & Clouet, P. The metabolism and availability of essential fatty acids in animal and human tissues. *Reprod Nutr Dev* **34**, 539-568 (1994).
54. Harmon, S.D., Kaduce, T.L., Manuel, T.D. & Spector, A.A. Effect of the Δ6-desaturase inhibitor SC-26196 on PUFA metabolism in human cells. *Lipids* **38**, 469-476 (2003).
55. Jump, D.B. & Clarke, S.D. Regulation of gene expression by dietary fat. *Annu Rev Nutr* **19**, 63-90 (1999).
56. Varga, T., Czimmerer, Z. & Nagy, L. PPARs are a unique set of fatty acid regulated transcription factors controlling both lipid metabolism and inflammation. *Biochim Biophys Acta* **1812**, 1007-1022 (2011).
57. Wahli, W. & Michalik, L. PPARs at the crossroads of lipid signaling and inflammation. *Trends Endocrinol Metab* **23**, 351-363 (2012).
58. Berger, J. & Wagner, J.A. Physiological and therapeutic roles of peroxisome proliferator-activated receptors. *Diabetes Technol Ther* **4**, 163-174 (2002).
59. Vega, R.B., Huss, J.M. & Kelly, D.P. The coactivator PGC-1 cooperates with peroxisome proliferator-activated receptor α in transcriptional control of nuclear genes encoding mitochondrial fatty acid oxidation enzymes. *Mol Cell Biol* **20**, 1868-1876 (2000).
60. Tang, C., Cho, H.P., Nakamura, M.T. & Clarke, S.D. Regulation of human Δ-6 desaturase gene transcription: identification of a functional direct repeat-1 element. *J Lipid Res* **44**, 686-695 (2003).
61. Kawashima, Y., Musoh, K. & Kozuka, H. Peroxisome proliferators enhance linoleic acid metabolism in rat liver. Increased biosynthesis of ω6 polyunsaturated fatty acids. *J Biol Chem* **265**, 9170-9175 (1990).

62. Schoonjans, K., Staels, B. & Auwerx, J. The peroxisome proliferator activated receptors (PPARS) and their effects on lipid metabolism and adipocyte differentiation. *Biochim Biophys Acta* **1302**, 93-109 (1996).
63. Kamei, Y. *et al.* PPARγ coactivator 1β/ERR ligand 1 is an ERR protein ligand, whose expression induces a high-energy expenditure and antagonizes obesity. *Proc Natl Acad Sci U S A* **100**, 12378-12383 (2003).
64. Blanquart, C., Barbier, O., Fruchart, J.C., Staels, B. & Glineur, C. Peroxisome proliferator-activated receptor alpha (PPARα) turnover by the ubiquitin-proteasome system controls the ligand-induced expression level of its target genes. *J Biol Chem* **277**, 37254-37259 (2002).
65. Genini, D. & Catapano, C.V. Control of peroxisome proliferator-activated receptor fate by the ubiquitinproteasome system. *J Recept Signal Transduct Res* **26**, 679-692 (2006).
66. Sengupta, S., Peterson, T.R., Laplante, M., Oh, S. & Sabatini, D.M. mTORC1 controls fasting-induced ketogenesis and its modulation by ageing. *Nature* **468**, 1100-1104 (2010).
67. Dibble, C.C. & Cantley, L.C. Regulation of mTORC1 by PI3K signaling. *Trends Cell Biol* **25**, 545-555 (2015).
68. Proud, C.G. Regulation of mammalian translation factors by nutrients. *Eur J Biochem* **269**, 5338-5349 (2002).
69. Wang, L., Lawrence, J.C., Sturgill, T.W. & Harris, T.E. Mammalian target of rapamycin complex 1 (mTORC1) activity is associated with phosphorylation of raptor by mTOR. *J Biol Chem* **284**, 14693-14697 (2009).
70. Park, S., Chun, S. & Kim, D. Cold exposure lowers energy expenditure at the cellular level. *Cell Biol Int* **37**, 638-642 (2013).
71. Al-Fageeh, M.B. & Smales, C.M. Control and regulation of the cellular responses to cold shock: the responses in yeast and mammalian systems. *Biochem J* **397**, 247-259 (2006).
72. Al-Fageeh, M.B., Marchant, R.J., Carden, M.J. & Smales, C.M. The cold-shock response in cultured mammalian cells: harnessing the response for the improvement of recombinant protein production. *Biotechnol Bioeng* **93**, 829-835 (2006).

6. Acknowledgments:

I would like to thank my mentor and supervisor Professor Akira Kakizuka for his guidance. I am thankful and truly appreciative of his support and kind encouragement. I would also like to thank Dr. Tomoki Yoshida for his supervision throughout this project, and for his friendship. I am very thankful to Professor James Hejna for his critical reading of the manuscript and guidance throughout. I extend my warm gratitude to my colleagues for their assistance and whom have all been a pleasure to work with.

This thesis is based on material contained in the following scholarly paper. Soaad Alfaqaan, Tomoki Yoshida, Hiromi Imamura, Chihiro Tsukano, Yoshiji Takemoto, Akira Kakizuka. PPARα-Mediated Positive-Feedback Loop Contributes to Cold Exposure Memory

[Scientific Reports, volume 9, issue 1, pages 4538, 2019]

DOI: 10.1038/s41598-019-40633-3

7. Supplementary Data

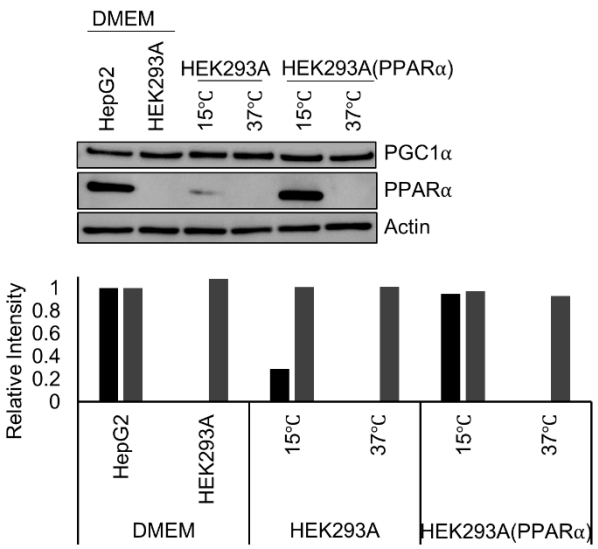

Supplementary Figure 1. Expression levels of PPARα and D6D in different culture conditions. Comparison of PPARα expression in HEK293A cells and HEK293A(PPARα) cells exposed to cold **(**15°C). All cells were collected at 24 h post-treatment (*n* = 3). All blots were derived from individual gels using the same samples. Values for HepG2 cells were set at 1. Error bars represent SD. For gel source data, see supplementary Data Fig. 2.

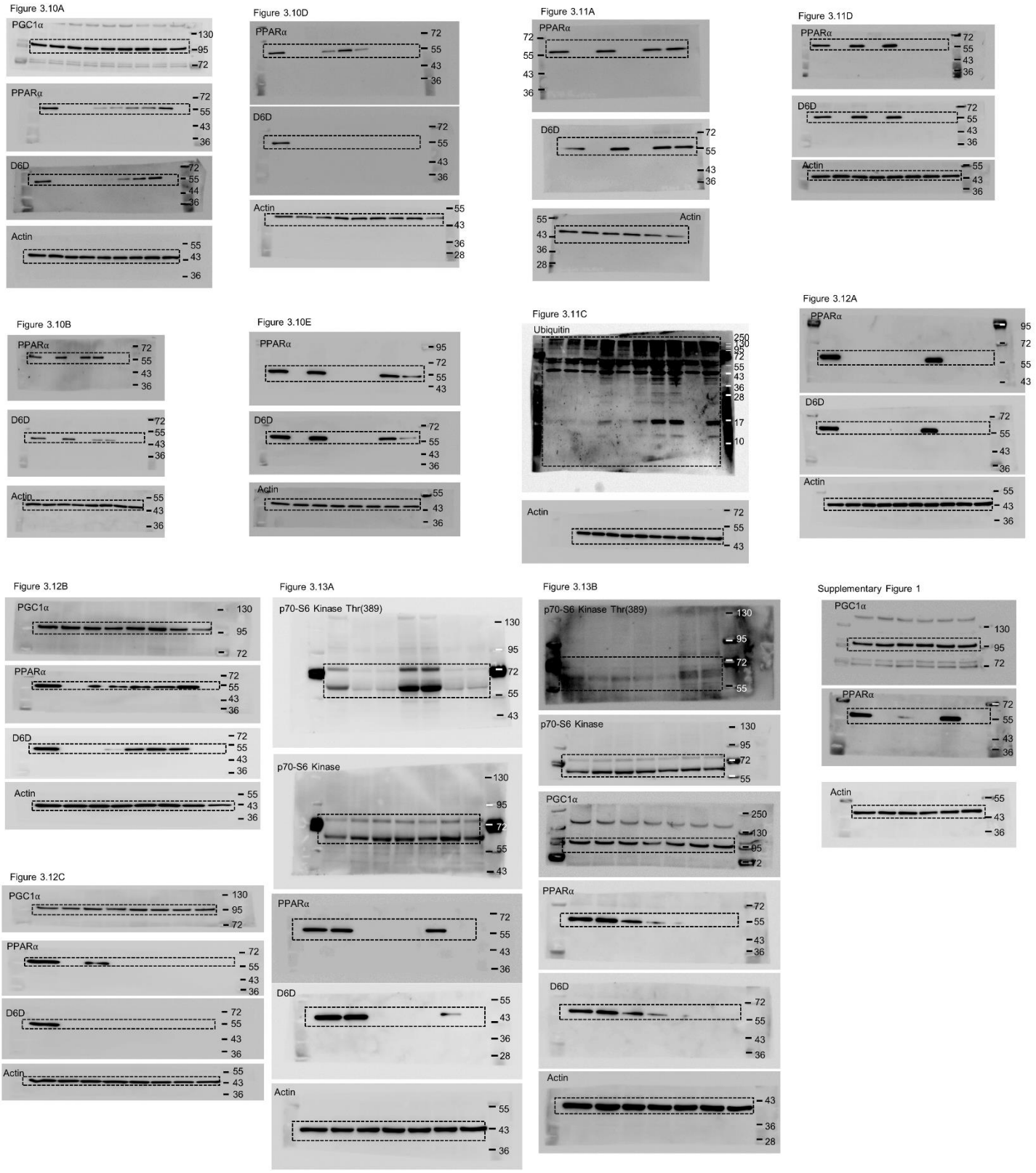

Supplementary Data Fig. 2. Unedited images of western blot analysis